NACA TN 4087

# NATIONAL ADVISORY COMMITTEE FOR AERONAUTICS

TECHNICAL NOTE 4087

## DROP-SIZE DISTRIBUTION FOR CROSSCURRENT BREAKUP OF LIQUID JETS IN AIRSTREAMS

By Robert D. Ingebo and Hampton H. Foster

Lewis Flight Propulsion Laboratory
Cleveland, Ohio



Washington
October 1957

NATIONAL ADVISORY COMMITTEE FOR AERONAUTICS

TECHNICAL NOTE 4087

# DROP-SIZE DISTRIBUTION FOR CROSSCURRENT BREAKUP OF LIQUID JETS IN AIRSTREAMS

By Robert D. Ingebo and Hampton H. Foster

4453

CN-1

## SUMMARY

Drop-size-distribution data were obtained for liquid jets atomized by cross-stream injection from simple orifices into high-velocity airstreams. A high-speed camera and a sampling technique were combined to obtain data over ranges of injector, liquid, and airstream variables. The volume-median drop diameter $D_{30}$ was calculated using the Rosin-Rammler, the log-probability, and the Nukiyama-Tanasawa distribution expressions. By means of dimensional analysis, the following empirical expression was obtained in correlating the ratio of the volume-median drop diameter to orifice diameter $D_{30}/D_o$ with the Weber-Reynolds number ratio $We/Re$:

$$D_{30}/D_o = 3.9(We/Re)^{0.25}$$

In the preceding equation, $We = \sigma/\rho_s D_o V_s^2$ and $Re = D_o V_s/\nu$ where $\sigma$ and $\nu$ are the surface tension and kinematic viscosity, respectively, of the liquid, and $V_s$ and $\rho_s$ are the free-stream velocity and density, respectively, of the air. A similar expression was obtained for the maximum drop diameter $D_{max}$ in each spray.

$$D_{max}/D_o = 22.3(We/Re)^{0.29}$$

From these expressions, the following modified Nukiyama-Tanasawa expression was derived for drop-size distribution:

$$\frac{dR}{dD} = 10^6\left(\frac{We}{Re}\right)^{0.24} \frac{D^5}{D_{max}^6} e^{-22.3(We/Re)^{0.04} D/D_{max}}$$

where $R$ is the volume fraction of drops having diameters $> D$. This expression utilizes a limiting maximum drop size and expresses drop-size distribution as a function of the dimensionless Weber-Reynolds number ratio.

## INTRODUCTION

The performance of jet engines is affected by the characteristics of the injection systems (refs. 1 and 2). Up to the present time, the atomization of the liquid, and the trajectory, acceleration, and vaporization of the droplets (ref. 3) have not been specifically related to engine performance. When a better understanding of all of these factors is obtained, then designing a fuel-injection system for optimum engine performance can be accomplished on a more scientific basis.

Several investigators (refs. 4 to 7) have obtained spray drop-size-distribution data, and as a result, equations have been derived which relate mean drop diameters to factors such as surface tension and air velocity. Although physical concepts of atomization have been developed, relatively few correlations of drop-size-distribution parameters with dimensionless force ratios have been made. This can be explained by the lack of equipment and instrumentation capable of giving accurate spray drop-size-distribution data which can be quickly analyzed.

In this investigation, a high-speed camera, capable of photographing microscopic droplets traveling at high velocities in airstreams (ref. 3), was used in combination with a sampling probe technique (ref. 8). By such a combination of photographic and sampling data, spray analyses could be speeded up and a large number of sprays tested in a relatively short time. Drop-size-distribution data were obtained by using simple orifice injectors oriented normal to the airflow. The breakup of fuel jets was investigated for ranges of injector, liquid, and airstream variables. Thus, atomization of liquid jets was studied under conditions similar to those for fuel atomization in ramjet engines and afterburners. Empirical expressions were derived from a dimensional analysis of the data.

## SYMBOLS

The following symbols are used in this report:

A integrated area for fuel distribution plot

a mean diameter notation

b constant

$C_o$ orifice discharge coefficient

c mean diameter notation

D droplet diameter, cm or microns

$D_o$ injector-orifice diameter, cm

$\overline{D}$ constant (eq. (2)), cm

$D^*$ constant (eq. (1)), cm

$D_{30}$ volume-median droplet diameter defined by the general expression

4453

$$(D_{ac})^{a-c} = \frac{\Sigma nD^a}{\Sigma nD^c} \quad \text{which gives} \quad D_{30} = (\Sigma nD^3/\Sigma n)^{1/3}$$

$l$ orifice length, cm

n number of droplets in given size range

q constant

R volume fraction of drops having diameters > D

Re Reynolds number based on orifice diameter, $D_oV_s/\nu$

V velocity, cm/sec

We Weber number, $\sigma/\rho_s V_s^2 D_o$

x vertical distance from injector orifice along spray centerline, in.

y $\ln(D/D^*)$

$\nu$ kinematic viscosity, $cm^2/sec$

$\mu$ absolute viscosity, gm/cm sec

$\rho$ density, g/cu cm

$\sigma$ surface tension, dynes/cm

Subscripts:

$l$ liquid

max observed maximum

o orifice

s free stream

t total

## APPARATUS AND PROCEDURE

The apparatus used to study the liquid-jet breakup in airstreams is shown in figures 1, 2, and 3 and described in detail in references 3 and 8. Velocity profiles in the 4- by 12-inch test section at the sampling station were relatively flat. For points up to within 1 inch of the walls, the variation was only between 2 and 4 percent, even at the highest air velocity. The air was preheated (250° to 900° F), when required, by a turbojet-engine combustor (fig. 1). The test liquids were isooctane (2,2,4-trimethylpentane), JP-5 fuel, water, benzene, and carbon tetrachloride. The liquid jets were directed at right angles to the airstream (fig. 2), from single plain orifices using pressurized nitrogen. The injector (fig. 3) was fabricated from an Inconel tube (diam. 1/2 in., wall, 1/16 in.) welded to the center of an Inconel plate (1/16" x 2" x 4") with the orifice at the center. The plate ends were beveled on the top side, and the orifices (0.010, 0.020, 0.030, and 0.040 in.) were drilled and reamed from the top side of the plate.

Photographs and sampling data were obtained by making vertical traverses along the spray centerline normal to the airstream and at a distance of 1±1/4 inch downstream from the injector. Vertical traverses made at distances of one inch on either side of the spray centerline showed no measurable effect of horizontal displacement on drop-size distribution. The high-speed camera, shown in figure 2 and described in reference 3, was used to obtain photomicrographs of the sprays (fig. 4). The sampling probe, shown in figure 2 and described in reference 8, was used for continuous sampling at airstream velocity. Isooctane and JP-fuel air samples of the sprays were passed through the NACA fuel-air mixture analyzer; from these data, spray-concentration profiles were determined. In the case of water sprays, a humidity meter was used to analyze the sample. Wet-bulb temperature measurements were obtained as described in reference 3 and used to determine benzene and carbon tetrachloride concentrations in the samples. Therefore, the analysis of the photographs gave droplet-size-distribution data, and the analysis of the probe samples gave data on liquid concentrations in the spray profile. Experimental test conditions and liquid properties are recorded in table I.

In the photomicrographs (fig. 4), the spray appears to be partially fractionated in the airstream inasmuch as the larger droplets tend to move out farther into the airstream than the smaller droplets because of the greater momentum of the larger droplets. Figure 5 shows typical spray-distribution curves for airstream velocities of 100, 180, and 300 feet per second. The 100-feet-per-second curve is replotted to a larger scale (fig. 6) in order to illustrate the method of analysis.

Since photomicrographs showed that the spray was partially fractionated in the airstream, the area under each spray-distribution curve was divided into area increments as shown in figure 6. Droplet counts were made for each increment and combined by means of sampling probe data to obtain the mean drop diameter $D_{30}$ as described in appendix A. Since the incremental areas contained size ranges considerably smaller than the overall size range, relatively few droplet measurements were made without incurring large statistical errors (i.e., > 3 percent). Also, the volume fraction of a given size in the entire spray was not determined directly by total droplet count. Instead, liquid concentrations were obtained from the sampling probe data and used in the final calculation of volume fractions. Thus, a relatively rapid method of size-distribution analysis was developed by combining the photographic and sampling techniques.

## RESULTS AND DISCUSSION

The log-probability, Rosin-Rammler, and Nukiyama-Tanasawa expressions for size distribution were used to determine the mean drop diameter $D_{30}$ for all of the experimental data in table I. A sample calculation of $D_{30}$ is given in appendix A. Also, experimental data and calculated values for each distribution equation are given in table II for three airstream-velocity conditions. The log-probability expression

$$1 - R = \frac{\delta}{\sqrt{\pi}} \int_{-\infty}^{\delta y} e^{-\delta^2 y^2} \, dy \qquad (1)$$

where $y = \ln(D/D^*)$, and $\delta$ is a constant used to plot data as shown in figure 7(a). Equation (1) predicts the probable existence of infinite-size drops whereas a maximum drop size was observed for each spray. Figure 7(a) shows that the data do not fall on single straight-line plots. Instead, curves were obtained which asymptotically approached a maximum size and make the determination of $D_{30}$ quite difficult (i.e., $\delta \neq$ a constant).

Figure 7(b) shows a plot of the following Rossin-Rammler expression:

$$R = e^{-(D/\overline{D})^q} \qquad (2)$$

Application of equation (2) for the calculation of $D_{30}$ was also found to be very difficult since values of $q = 3$ were obtained. This difficulty arises when the slope of the plot $q$ approaches 3, and $D_{30}$ approaches zero. A similar result was noted in reference 7.

Best results were obtained with the Nukiyama-Tanasawa expression:

$$dR/dD = \frac{b^6}{120} D^5 e^{-bD} \qquad (3)$$

Figures 7(c) and 8 show that $D_{30}$ (as determined from eq. (3)) decreases as airstream velocity increases and is affected very little when both liquid and air temperature are increased. Even though equation (3) predicts infinitely large drops, straight-line plots were obtained for the entire distribution of sizes. Thus, equation (3) was used to calculate $D_{30}$ for each test condition, and results are recorded in table III.

Tests were first made to determine the effect of injection conditions (liquid-jet velocity $V_l$, orifice discharge coefficient $C_o$, and the length-diameter ratio for the orifice $l/D_o$) on the mean drop diameter $D_{30}$. A sample of results is given in the following table for three values of airstream velocity $V_s$ and a constant orifice diameter $D_o$ of 0.02 inch. Airstream temperature and static pressure were approximately constant at 90° F and 29.3 inches of mercury, respectively.

| $V_l$, ft/sec | $C_o$ | $l/D_o$ | $D_{30}$ |
|---|---|---|---|
| $V_s$, 300 ft/sec | | | |
| 182 | 0.87 | 1.00 | 32 |
| 80 | .86 | 1.00 | 31 |
| 84 | .89 | 4.65 | 33 |
| $V_s$, 180 ft/sec | | | |
| 204 | 0.88 | 4.65 | 47 |
| 84 | .89 | 4.65 | 49 |
| 81 | .77 | 1.00 | 47 |
| $V_s$, 100 ft/sec | | | |
| 81 | 0.77 | 1.00 | 69 |
| 80 | .86 | 1.00 | 68 |

These data indicate relatively little effect of liquid-jet velocity, orifice discharge coefficient, and length-diameter ratio on the mean drop diameter $D_{30}$. This result appeared to be explained by the fact that the force of the airstream was normal to the liquid jet. Therefore, the only remaining injector variable to be considered is the orifice diameter $D_o$. The effect of this variable was then studied together with liquid properties and airstream conditions with the aid of dimensional analysis.

The mean drop diameter $D_{30}$, produced by cross-stream breakup of liquid jets in airstreams, is to be considered a function of the orifice diameter, liquid properties, and airstream conditions. Then the following expression is obtained:

$$D_{30} = \varphi(D_o,\rho_l,V_s,\sigma,\mu_l,\rho_s,\mu_s) \tag{4}$$

By rewriting equation (4), there results

4453

$$D_{30} = \alpha(D_o)^a(\rho_l)^b(V_s)^c(\sigma)^d(\mu_l)^e(\rho_s)^f(\mu_s)^g \tag{5}$$

where $\alpha$ is a proportionality constant. By means of dimensional analysis (appendix B) we obtain

$$\frac{D_{30}}{D_o} = \alpha\left(\frac{\sigma}{D_o\rho_l V_s^2}\right)^d \left(\frac{\mu_l}{D_o\rho_l V_s}\right)^{g+e} \left(\frac{\rho_s}{\rho_l}\right)^f \left(\frac{\mu_s}{\mu_l}\right)^g \tag{6}$$

which combines the seven variables assumed to influence $D_{30}$ into four dimensionless groups.

To determine the proportionality constant $\alpha$ and the four exponents d, e, f, and g, the effect of airstream static pressure on $D_{30}$ was investigated first because it appears only in the ratio $\rho_s/\rho_l$ and has a negligible effect on $\mu_s$. A plot of $D_{30}$ against airstream static pressure is shown in figure 9, and the exponent f was found to be -1/4. Thus, equation (6) becomes

$$\frac{D_{30}}{D_o}\left(\frac{\rho_s}{\rho_l}\right)^{1/4} = \alpha\left(\frac{\sigma}{D_o\rho_l V_s^2}\right)^d \left(\frac{\mu_l}{D_o\rho_l V_s}\right)^{g+e} \left(\frac{\mu_s}{\mu_l}\right)^g \tag{7}$$

Airstream static pressure was not treated further as a separate variable.

The exponent d was determined by making tests with $(\mu_l/D_o\rho_l V_s)$ held approximately constant at several constant values of the viscosity ratio $\mu_s/\mu_l$ and by varying the remaining groups. A plot of these data are shown in figure 10. In figure 10 a single straight-line plot is obtained which gives the exponent d a value of 1/4. The exponent g is approximately zero since no appreciable effect was observed when $\mu_s/\mu_l$ was varied by a factor of 3.

Thus, equation (7) becomes

$$\frac{D_{30}}{D_o}\left(\frac{D_o \rho_s V_s^2}{\sigma}\right)^{1/4} = \alpha\left(\frac{\mu_l}{D_o \rho_l V_s}\right)^e = \alpha\left(\frac{\nu}{D_o V_s}\right)^e \tag{8}$$

where $(\sigma/D_o \rho_s V_s^2)$ is commonly referred to as the Weber number or the ratio of surface tension to the turbulent momentum-transfer force of the airstream. The group $(D_o V_s/\nu)$ is actually a liquid-film Reynolds number. Since the effect of air viscosity was found negligible, liquid-film resistance appeared to control the breakup process. Also, both the Weber and Reynolds numbers were based on the orifice diameter $D_o$ as the characteristic length, and the velocity difference or relative velocity in each case is the airstream velocity $V_s$ for cross-stream injection.

Thus, equation (8) may be rewritten as

$$\frac{D_{30}}{D_o} We^{-1/4} = \alpha \; Re^{-e} \tag{9}$$

A total of 43 tests were completed, recorded in table III, and plotted in figure 11. Results showed that $e = 1/4$, and from figure 12 it was found that $\alpha = 3.9$.

Substitution of values for $e$ and $\alpha$ into equation (9) gives

$$\frac{D_{30}}{D_o} = 3.9(We/Re)^{0.25} \tag{10}$$

A comparison of equation (10) with results obtained from other methods of atomization is given in table IV.

If the maximum drop diameter $D_{max}$ is also assumed to be a function of the properties given in equation (4), from dimensional analysis and figure 13, the result is that

$$\frac{D_{max}}{D_o} = 22.3(We/Re)^{0.29} \tag{11}$$

Thus, empirical expressions were obtained which gave relations between the mean drop diameter $D_{30}$, or maximum drop diameter $D_{max}$ and the Weber-Reynolds number ratio.

4453

CN-2

The Nukiyama-Tanasawa distribution expression (eq. (3)) does not recognize the existance of a maximum drop size in a spray. However, by determining a relation between $D_{30}$ calculated by equation (11) and the maximum drop diameter $D_{max}$, a modified expression for size distribution can be obtained. By combining equations (10) and (11), the following equation is obtained:

$$\frac{D_{max}}{D_{30}} = 5.7(We/Re)^{0.04} \tag{12}$$

which agrees with figure 14. Since $D_{30} = 3.915/b$, equation (3) may be rewritten

$$\frac{dR}{dD} = 10^6 \left(\frac{We}{Re}\right)^{0.24} \frac{D^5}{D_{max}^6} e^{-22.3\left(\frac{We}{Re}\right)^{0.04} \frac{D}{D_{max}}} \tag{13}$$

All of the drop-size-distribution data were tested using equation (13), and the results were good. A sample is shown in figure 15 where $\log \Delta R_t D_{max}^6/(\Delta D)D^5$ is plotted against $D/D_{max}$ as calculated from tables II and III. Figure 15 shows that the data agree fairly well with the straight line predicted by equation (13). Thus, an expression was obtained which shows the effect of the maximum drop diameter and the Weber-Reynolds number ratio on the complete size distribution.

## CONCLUSIONS

The breakup of liquid jets injected cross-stream into high velocity airstreams conformed reasonably well to the following modified Nukiyama-Tanasawa expression for drop-size distribution:

$$\frac{dR}{dD} = 10^6 \frac{D^5}{D_{max}^6} (We/Re)^{0.24} e^{-22.3\left(\frac{We}{Re}\right)^{0.04} \frac{D}{D_{max}}}$$

Also, the empirical expressions

$$D_{30} = 3.9\ D_o(We/Re)^{0.25}$$

and

$$D_{max} = 22.3\ D_o(We/Re)^{0.29}$$

were found to give good correlations of the observed maximum drop diameter $D_{max}$, or the mean drop diameter $D_{30}$ with the orifice diameter $D_o$ and the Weber-Reynolds number ratio.

Lewis Flight Propulsion Laboratory
National Advisory Committee for Aeronautics
Cleveland, Ohio, June 11, 1957

4453

# APPENDIX A

## SAMPLE CALCULATION OF MEAN DROP DIAMETER $D_{30}$

The incremental volume function $\Delta R_i$ for each incremental area $\Delta A_i$ may be expressed as

$$\Delta R_i = n_i D^3 / \Sigma n_i D^3$$

In the first area increment (i = 1, table II) D equals 15, 25, 40,
4453 50, and 65 microns. The corresponding number of drops n for each size was 0, 120, 80, 0, and 7, therefore,

$$n_i D^3 = 0,\ 1.88 \times 10^6,\ 5.18 \times 10^6,\ 0,\ \text{and}\ 1.92 \times 10^6\ (\text{microns}^3)$$

respectively, and

$$\sum_{D=15}^{D=65} n_i D^3 = 8.98 \times 10^6\ (\text{microns}^3)$$

so that

$$\Delta R_i = \frac{n_i D^3}{\sum_{D=15}^{D=65} n_i D^3} = 0,\ 0.208,\ 0.578,\ 0,\ \text{and}\ 0.214$$

The volume fraction for a given drop size in an area increment is $\Delta R_i$; $\Delta R_2$, $\Delta R_3$, $\Delta R_4$, and $\Delta R_5$ may be calculated in a similar manner.

The value of $\Delta R_t$ for a given drop size may be expressed as

$$\Delta R_t = \sum_{i=1}^{i=5} \Delta R_i \frac{\Delta A_i}{A}$$

For example, in table II, $A = \sum_{i=1}^{i=5} \Delta A_i = 0.0469$

And when D equals 15 microns,

$$\Delta R_t = \sum_{i=1}^{i=5} \Delta R_i \frac{\Delta A_i}{A} = 0 + \Delta R_2 \left(\frac{\Delta A_2}{A}\right) + 0 + 0 + 0 = 0.001 \frac{0.01032}{0.0469} = 0.0002$$

where $\Delta A_i/A$ is the weight or volume fraction of drops for a given area increment, and $\Delta R_t$ is the total volume fraction for a given drop size in the entire spray.

The term $R$ is defined as the volume fraction of drops having diameters $> D$. Thus, for $D > 15$ microns, $R = 1$, and for $D > 225$ microns, $R = 0.0257 = \Delta R_t$.

The Nukiyama-Tanasawa expression

$$\frac{dR}{dD} = \frac{b^6/\beta}{\Gamma(6/\beta)} D^5 e^{-bD^\beta}$$

(where $\beta$ is a constant) may be written as follows:

$$\log \frac{\Delta R_t}{(\Delta D)D^5} = -\frac{bD^\beta}{2.3} + \log \frac{b^6}{\beta\Gamma(6/\beta)}$$

Plots of $\log \left(\Delta R_t/(\Delta D)D^5\right)$ against $D$ were made for all of the experimental drop-size-distribution data, and best results were obtained when $\beta = 1$. Thus, equation (3), $dR/dD = (b^6/120)\, D^5 e^{-bD}$, was obtained, which may be rewritten as follows:

$$\log \frac{\Delta R_t}{(\Delta D)D^5} = -\frac{b}{2.3} D + \log \frac{b^6}{120}$$

where $-(b/2.3)$ is the slope of the plot in figures 7(c) or 8. Integration of the preceding expression yields the following general expression for mean drop sizes:

$$D_{ac}^{a-c} = b^{-(a-c)}\Gamma(a + 3)/\Gamma(c + 3)$$

Thus, the equation for $D_{30}$ ($a = 3$, and $c = 0$) becomes

$$D_{30}^3 = b^{-3}\Gamma 6/\Gamma 3$$

or

$$D_{30} = 3.915/b$$

Other mean drop diameters may be readily obtained from the general expression for mean drop sizes. In figure 6(c), the slope of the plot for $V_s$ = 300 feet per second is

$$\text{slope} = \frac{-12.3 + 8.1}{100} = -0.042 = -\frac{b}{2.3}$$

thus,

$$D_{30} = 3.915/(2.3)(0.042) = 40.5 \text{ microns}$$

# APPENDIX B

## DIMENSIONAL ANALYSIS

When equation (5) is rewritten, the following expression results:

$$D_{30} = \alpha(D_o)^a(\rho_l)^b(V_s)^c(\sigma)^d(\mu_l)^e(\rho_s)^f(\mu_s)^g$$

The preceding equation is then expressed in terms of the mass-length-time system (where $T$ is time; M, mass; and $l$, length) to give

$$l = \alpha(l)^a\left(\frac{M}{l^3}\right)^b\left(\frac{l}{T}\right)^c\left(\frac{M}{T^2}\right)^d\left(\frac{M}{lT}\right)^e\left(\frac{M}{l^3}\right)^f\left(\frac{M}{lT}\right)^g$$

so that for

$$\Sigma M, \qquad 0 = b + d + e + f + g$$

$$\Sigma l, \qquad 1 = a - 3b + c - e - 3f - g$$

$$\Sigma T, \qquad 0 = -c - 2d - e - g$$

which may be rewritten as

$$a = 1 - d - e - g$$

$$b = -d - e - f - g$$

$$c = -2d - e - g$$

Substitution of these values into equation (5) gives

$$\frac{D_{30}}{D_o} = \left(\frac{\sigma}{V_s^2\rho_l D_o}\right)^d\left(\frac{\mu_l}{\rho_l D_o V_s}\right)^{g+e}\left(\frac{\rho_s}{\rho_l}\right)^f\left(\frac{\mu_s}{\mu_l}\right)^g$$

which is equation (6).

4453

## REFERENCES


1. Sharp, J. G.: Effects of Fuel Type on the Performance of Aero-Gas Turbine Combustion Chambers, and the Influence of Design Features. Jour. Roy. Aero. Soc., vol. 58, no. 528, Dec. 1954, pp. 813-825.

2. The Staff of the National Gas Turbine Establishment: The Correlation of Combustion Efficiency and Injector Characteristics Under Simulated Altitude Idling Conditions. Combustion Res. and Rev., Butterworths Sci. Pub. (London), 1955, pp. 53-57.

3. Ingebo, Robert D.: Vaporization Rates and Drag Coefficients for Isooctane Sprays in Turbulent Air Streams. NACA TN 3265, 1954.

4. Nukiyama, Shirō, and Tanasawa, Yasushi (E. Hope, Trans.): Experiments on the Atomization of Liquids in an Air Stream. Rep. No. 3, On the Droplet-Size Distribution in an Atomized Jet, Defence Res. Board, Dept. Nat. Defence, Ottawa (Canada), Mar. 18, 1950. (Trans. from Trans. Soc. Mech. Eng. (Japan), vol. 5, no. 18, Feb. 1939, pp. 62-67.)

5. Conroy, E. H., and Johnstone, H. F.: Combustion of Sulfur in a Venturi Spray Burner. Ind. and Eng. Chem., vol. 41, no. 12, 1949, pp. 2741-2748.

6. Longwell, J. P.: Fuel Oil Atomization. D.Sc. Thesis, M.I.T., 1943.

7. Bowen, I. G., and Joyce, J. R.: The Effects of Cone Angle, Pressure and Flow Number on the Particle Size of a Pressure Jet Atomiser. Tech. Rep. No. I.C.T./17, The Shell Petroleum Co., Ltd. (London), Mar. 15, 1948.

8. Foster, Hampton H., and Ingebo, Robert D.: Evaporation of JP-5 Fuel Sprays in Air Streams. NACA RM E55K02, 1956.

9. Turner, G. M., and Moulton, R. W.: Drop Size Distributions from Spray Nozzles. Chem. Eng. Prog., vol. 49, no. 4, Apr. 1953, pp. 185-190.

4453

TABLE I. - TEST CONDITIONS FOR CROSS-STREAM BREAKUP OF LIQUID JETS

| Run | Injector orifice diameter, in. | Air-stream velocity, ft/sec | Air temperature, °F | Air pressure, in. Hg abs | Air density, lb/cu ft | Liquid jet velocity, ft/sec | Liquid temperature, °F | Liquid density, lb/cu ft | Liquid viscosity, millipoises | Surface tension, dynes/cm |
|---|---|---|---|---|---|---|---|---|---|---|
| Isooctane | | | | | | | | | | |
| 1 | 0.010 | 100 | 89 | 29.3 | 0.071 | 180 | 88 | 42.6 | 4.75 | 20.7 |
| 2 | .020 | | 87 | | .071 | 80 | 91 | | | |
| 3 | .020 | | 85 | | .071 | 81 | 94 | | | |
| 4 | .030 | ↓ | 88 | ↓ | .071 | 51 | 93 | | | |
| 5 | .030 | 180 | 90 | 20 | .048 | 76 | 82 | | | |
| 6 | .040 | | 86 | 29.3 | .071 | 59 | 90 | | | |
| 7 | .020 | | 90 | | .071 | 80 | 93 | | | |
| 8 | | | 85 | | .071 | 81 | 94 | | | |
| 9 | | | 85 | | .071 | 84 | 88 | | | |
| 10 | ↓ | | 87 | | .071 | 204 | 86 | | | |
| 11 | .030 | | 87 | | .071 | 51 | 92 | ↓ | ↓ | ↓ |
| 12 | | | 87 | | .071 | 51 | 198 | 40.0 | 2.85 | 16.0 |
| 13 | | | 82 | | .072 | 54 | 82 | 42.6 | 4.75 | 20.7 |
| 14 | | | 80 | ↓ | .072 | 76 | 80 | | | |
| 15 | | | 80 | 50 | .123 | 76 | 83 | | | |
| 16 | ↓ | | 82 | 29.3 | .071 | 76 | 82 | ↓ | ↓ | ↓ |
| 17 | .020 | | 300 | | .051 | 83 | 150 | 40.0 | 2.85 | 16.0 |
| 18 | .030 | | 900 | | .029 | 51 | 200 | | | |
| 19 | .020 | ↓ | 900 | | .029 | 82 | 174 | ↓ | ↓ | ↓ |
| 20 | | 300 | 87 | | .071 | 80 | 93 | 42.6 | 4.75 | 20.7 |
| 21 | | | 87 | | .071 | 182 | 82 | | | |
| 22 | ↓ | | 87 | | .071 | 84 | 94 | | | |
| 23 | .030 | | 85 | | .071 | 51 | 85 | | | |
| 24 | .040 | ↓ | 86 | | .071 | 58 | 88 | | | |
| 25 | .030 | 350 | 900 | | .029 | 51 | 98 | ↓ | ↓ | ↓ |
| 26 | | 352 | 900 | | .029 | 80 | 186 | 40.0 | 2.85 | 16.0 |
| 27 | | 700 | 900 | | .029 | 42 | 200 | | | |
| 28 | ↓ | 700 | 900 | ↓ | .029 | 79 | 150 | ↓ | ↓ | ↓ |
| JP-5 Fuel | | | | | | | | | | |
| 29 | 0.030 | 180 | 80 | 29.3 | 0.071 | 54 | 80 | 51.1 | 15.8 | 28.5 |
| 30 | .030 | 300 | 80 | 29.3 | .071 | 54 | 80 | 51.1 | 15.8 | 28.5 |
| Benzene | | | | | | | | | | |
| 31 | 0.030 | 352 | 900 | | 0.029 | 53.5 | 150 | 52.0 | 3.7 | 22.6 |
| 32 | .030 | 700 | 900 | 29.7 | .029 | 53.5 | 145 | 52.0 | 3.8 | 23.0 |
| Carbon tetrachloride | | | | | | | | | | |
| 33 | | 180 | 86 | 29.3 | 0.071 | 35.5 | 87 | 99.5 | 8.4 | 25.2 |
| 34 | | 300 | 86 | 29.3 | .071 | 35.5 | 87 | 99.5 | 8.4 | 25.2 |
| Water | | | | | | | | | | |
| 35 | 0.020 | 100 | 86 | 29.3 | 0.071 | 70 | 76 | 62.4 | 8.4 | 71.0 |
| 36 | | 180 | 82 | | .071 | 73 | 90 | 62.4 | 8.4 | 71.0 |
| 37 | | | 900 | | .029 | 73 | 140 | 62.3 | 4.70 | 66.2 |
| 38 | | | 250 | | .055 | 72.5 | 140 | | | |
| 39 | | ↓ | 250 | | .055 | 70 | | | | |
| 40 | | 350 | 900 | ↓ | .029 | 72.5 | | | | |
| 41 | ↓ | 700 | | 29.9 | .029 | 70 | ↓ | | ↓ | ↓ |
| 42 | .030 | 300 | 84 | 29.3 | .071 | 48.2 | 99 | | 8.4 | 71.0 |
| 43 | | 180 | | | | 48.2 | | ↓ | | |

TABLE II. - SAMPLE DROP-SIZE-DISTRIBUTION DATA AND CALCULATIONS FOR ISOOCTANE SPRAY

[Jet stream velocity, 51 ft/sec; jet density, 42.6 lb/cu ft; orifice diameter, 0.030 in.; downstream distance from injector, 1±1/4 in.]

(a) Run 4; airstream velocity, 100 ft/sec; air temperature, 88° F; air pressure, 29.3 in. Hg abs

| Distance[a] from orifice, x, in. | | 0 to 1.5 | | 1.5 to 2.1 | | 2.1 to 2.5 | | 2.5 to 2.9 | | 2.9 to 3.5 | | $\Delta R_t$ | Volume fraction of drops having diameter > D, R | $\text{Log}\ \frac{1}{R}$ (c) | $\text{Log}\ \frac{\Delta R}{(\Delta D)D^5}$ (d) | 100 (1-R) (e) | Log D (e) |
|---|---|---|---|---|---|---|---|---|---|---|---|---|---|---|---|---|---|
| Area increment[a], $\Delta A$ | | 0.00327 | | 0.01032 | | 0.01372 | | 0.01413 | | 0.00548 | | | | | | | |
| Drop diameter, D, microns: Range | Average | $n_1$ (b) | $\Delta R_1$ | $n_2$ | $\Delta R_2$ | $n_3$ | $\Delta R_3$ | $n_4$ | $\Delta R_4$ | $n_5$ | $\Delta R_5$ | | | | | | |
| 7.5 - 20 | 15 | 0 | 0 | 60 | 0.001 | 0 | 0 | 0 | 0 | 0 | 0 | 0.0002 | 1.0000 | 0 | -10.506 | 0 | 1.176 |
| 20 - 32.5 | 25 | 120 | .208 | 575 | .060 | 22 | .003 | 0 | 0 | 0 | 0 | .0285 | .9997 | .0001 | -9.632 | .03 | 1.398 |
| 32.5 - 45 | 40 | 81 | .578 | 193 | .082 | 45 | .007 | 0 | 0 | 0 | 0 | .0603 | .9712 | .0127 | -10.327 | 2.88 | 1.602 |
| 45 - 57.5 | 50 | 0 | 0 | 193 | .161 | 83 | .024 | 15 | .006 | 0 | 0 | .0441 | .9109 | .0405 | -10.948 | 8.91 | 1.699 |
| 57.5 - 70 | 65 | 7 | .214 | 64 | .117 | 49 | .031 | 4 | .003 | 3 | .006 | .0515 | .8668 | .0621 | -11.450 | 13.32 | 1.813 |
| 70 - 82.5 | 75 | 0 | 0 | 23 | .065 | 40 | .039 | 7 | .009 | 6 | .018 | .0305 | .8154 | .0886 | -11.989 | 18.46 | 1.875 |
| 82.5 - 95 | 90 | | | 34 | .165 | 52 | .087 | 11 | .024 | 7 | .037 | .0735 | .7849 | .1052 | -12.001 | 21.51 | 1.954 |
| 95 - 107.5 | 100 | | | 13 | .087 | 38 | .087 | 10 | .030 | 6 | .044 | .0589 | .7114 | .1479 | -12.327 | 28.86 | 2.000 |
| 107.5 - 120 | 115 | | | 10 | .100 | 19 | .066 | 20 | .092 | 3 | .033 | .0735 | .6525 | .1855 | -12.534 | 34.76 | 2.060 |
| 120 - 132.5 | 125 | | | 5 | .065 | 36 | .161 | 25 | | 4 | .059 | .1130 | .5790 | .2373 | -12.528 | 42.10 | 2.097 |
| 132.5 - 145 | 140 | | | 2 | .037 | 18 | .113 | 15 | .125 | 3 | .061 | .0860 | .4660 | .3316 | -12.893 | 53.40 | 2.146 |
| 145 - 157.5 | 150 | | | 1 | .023 | 10 | .078 | 8 | .082 | 0 | 0 | .0523 | .3800 | .4202 | -13.259 | 62.00 | 2.176 |
| 157.5 - 170 | 165 | | | 0 | 0 | 6 | .062 | 10 | .137 | 3 | .099 | .0708 | .3277 | .4845 | -13.334 | 67.23 | 2.217 |
| 170 - 182.5 | 175 | | | 1 | .036 | 9 | .111 | 7 | .114 | 2 | .079 | .0838 | .2569 | .5902 | -13.389 | 74.31 | 2.243 |
| 182.5 - 195 | 190 | | | 0 | | 5 | .079 | 7 | .146 | 3 | .152 | .0847 | .1731 | .7617 | -13.568 | 82.69 | 2.279 |
| 195 - 207.5 | 200 | | | | | 0 | 0 | 2 | .049 | 2 | .118 | .0284 | .0884 | 1.0538 | -14.148 | 91.16 | 2.301 |
| 207.5 - 220 | 215 | | | | | 0 | 0 | 0 | 0 | 4 | .294 | .0343 | .0600 | 1.2224 | -14.224 | 94.01 | 2.332 |
| 220 - 232.5 | 225 | | | | | 2 | .0523 | 1 | .035 | 0 | 0 | .0257 | .0257 | 1.5906 | -14.448 | 97.43 | 2.352 |

[a]Fig. 5

[b]Number of drops n.

[c]Fig. 6(b).

[d]Figs. 6(c) and 7; $\Delta D$ = 12.5 microns.

[e]Fig. 6(a).

4453

TABLE II. - Concluded. SAMPLE DROP-SIZE-DISTRIBUTION DATA AND CALCULATIONS FOR ISOOCTANE SPRAY

[Jet stream velocity, 51 ft/sec; jet density, 42.6 lb/cu ft; orifice diameter, 0.030 in.; downstream distance from injector, 1±1/4 in.]

(b) Run 11; airstream velocity, 180 ft/sec; air density, 0.072 lb/cu ft

| Distance from orifice, x, in. | | 0 to 1.0 | | 1.0 to 1.9 | | $\Delta R_t$ | Volume fraction of drops having diameter >D, R | $\log \frac{1}{R}$ | $\log \frac{\Delta R}{(\Delta D)D^5}$ | 100 (1-R) | Log D |
|---|---|---|---|---|---|---|---|---|---|---|---|
| Area increment, $\Delta A$ | | 0.01394 | | 0.0597 | | | | | | | |
| Drop diameter, D, microns | | $n_1$ | $\Delta R_1$ | $n_2$ | $\Delta R_2$ | | | | | | |
| Range | Average | | | | | | | (a) | (b) | (c) | (c) |
| 5 - 17.5 | 15 | 950 | 0.045 | 120 | 0 | 0.0095 | 1.00 | 0 | -9.000 | 0 | 1.176 |
| 17.5 - 30 | 25 | 611 | .135 | 70 | .003 | .0280 | .9905 | .0041 | -9.639 | .95 | 1.398 |
| 30 - 42.5 | 40 | 315 | .285 | 30 | .006 | .0583 | .9625 | .0166 | -10.342 | 3.75 | 1.607 |
| 42.5 - 55 | 50 | 173 | .305 | 170 | .061 | .1068 | .9042 | .0438 | -10.563 | 9.58 | 1.699 |
| 55 - 67.5 | 65 | 38 | .147 | 129 | .101 | .1095 | .7974 | .0983 | -11.122 | 20.26 | 1.813 |
| 67.5 - 80 | 75 | 4 | .024 | 117 | .140 | .1183 | .6878 | .1625 | -11.399 | 31.22 | 1.875 |
| 80 - 92.5 | 90 | 3 | .031 | 83 | .172 | .1453 | .5695 | .2445 | -11.706 | 43.05 | 1.954 |
| 92.5 - 105 | 100 | 2 | .028 | 66 | .188 | .1575 | .4242 | .3724 | -11.900 | 57.58 | 2.000 |
| 105 - 117.5 | 115 | 0 | 0 | 33 | .143 | .1157 | .2667 | .5740 | -12.337 | 73.33 | 2.060 |
| 117.5 - 130 | 125 | | | 21 | .117 | .0946 | .1510 | .8210 | -12.606 | 84.90 | 2.097 |
| 130 - 142.5 | 140 | | | 4 | .031 | .0253 | .0564 | 1.2484 | -13.424 | 94.36 | 2.146 |
| 142.5 - 155 | 150 | | | 4 | .038 | .0311 | .0311 | 1.5068 | -13.484 | 96.89 | 2.176 |

(c) Run 23; airstream velocity, 300 ft/sec; air density, 0.072 lb/cu ft

| Distance from orifice, x, in. | | 0 to 0.4 | | 0.4 to 0.9 | | $\Delta R_t$ | Volume fraction of drops having diameter >D, R | $\log \frac{1}{R}$ | $\log \frac{\Delta R}{(\Delta D)D^5}$ | 100 (1-R) | Log D |
|---|---|---|---|---|---|---|---|---|---|---|---|
| Area increment, $\Delta A$ | | 0.01514 | | 0.06473 | | | | | | | |
| Drop diameter, D, microns | | $n_1$ | $\Delta R_1$ | $n_2$ | $\Delta R_2$ | | | | | | |
| Range | Average | | | | | | | (a) | (b) | (c) | (c) |
| 5 - 17.5 | 15 | 48 | 0.084 | 30 | 0.004 | 0.0187 | 1.000 | 0 | -8.705 | 0 | 1.176 |
| 17.5 - 30 | 25 | 20 | .162 | 80 | .043 | .0656 | .9813 | .0083 | -9.270 | 1.87 | 1.398 |
| 30 - 42.5 | 40 | 6 | .199 | 55 | .121 | .1360 | .9157 | .0383 | -9.974 | 8.43 | 1.602 |
| 42.5 - 55 | 50 | 3 | .194 | 36 | .155 | .1625 | .7797 | .1081 | -10.381 | 22.03 | 1.699 |
| 55 - 67.5 | 65 | 1 | .142 | 17 | .161 | .1573 | .6172 | .2096 | -10.965 | 38.28 | 1.813 |
| 67.5 - 80 | 75 | 1 | .219 | 11 | .160 | .1710 | .4599 | .3373 | -11.239 | 54.01 | 1.875 |
| 80 - 92.5 | 90 | 0 | 0 | 8 | .201 | .1628 | .2889 | .5393 | -11.656 | 71.11 | 1.954 |
| 92.5 - 105 | 100 | | | 3 | .103 | .0837 | .1261 | .8993 | -12.174 | 87.39 | 2.000 |
| 105 - 117.5 | 115 | | | 1 | .052 | .0425 | .0423 | 1.3732 | -12.772 | 95.77 | 2.061 |

[a] Fig. 6(b).

[b] Figs. 6(c) and 7.

[c] Fig. 6(a).

4453

TABLE III. - MAXIMUM DROP SIZE $D_{max}$, MEAN DROP SIZE $D_{30}$, AND DIMENSIONLESS FORCE RATIOS

| Run | $D_{max}$ | $D_{30}$ | Weber number, We, $\frac{\sigma}{V_s^2 \rho_s D_o}$ | Reynolds number, Re, $\frac{D_o V_s}{\nu}$ | We/Re | $D_{30}/D_o$ | $\left(\frac{We}{Re}\right)^{0.25}$ | $\frac{D_{max}}{D_{30}}$ |
|---|---|---|---|---|---|---|---|---|
| | | | | Isooctane | | | | |
| 1 | 175 | 55 | $77.4\times10^{-3}$ | 11,100 | $6.95\times10^{-6}$ | 0.216 | 0.052 | 3.20 |
| 2 | 225 | 68 | 38.6 | 22,300 | 1.735 | .134 | .036 | 3.30 |
| 3 | 190 | 69 | 38.5 | 22,300 | 1.72 | .137 | .036 | 2.74 |
| 4 | 225 | 81 | 25.8 | 33,900 | .76 | .106 | .020 | 2.79 |
| 5 | 175 | 65 | 11.7 | 60,000 | .194 | .0856 | .021 | 2.68 |
| 6 | 190 | 62 | 5.9 | 80,300 | .074 | .0609 | .010 | 3.07 |
| 7 | 150 | 47 | 11.9 | 40,100 | .299 | .0927 | .020 | 3.18 |
| 8 | 140 | 47 | 11.9 | 40,100 | .296 | .0927 | .023 | 2.97 |
| 9 | 150 | 49 | 11.9 | 40,100 | .296 | .0955 | .023 | 3.09 |
| 10 | 140 | 47 | 11.9 | 40,100 | .297 | .0927 | .023 | 2.97 |
| 11 | 150 | 52 | 7.9 | 60,000 | .130 | .0745 | .019 | 2.64 |
| 12 | 140 | 47 | 6.1 | 93,600 | .065 | .0620 | .016 | 2.96 |
| 13 | 140 | 55 | 7.9 | 60,000 | .131 | .0720 | .019 | 2.56 |
| 14 | 140 | 53 | 7.9 | 60,000 | .131 | .0696 | .019 | 2.64 |
| 15 | 140 | 51 | 4.6 | 60,000 | .076 | .0665 | .017 | 2.76 |
| 16 | 140 | 50 | 7.9 | 60,000 | .131 | .0720 | .019 | 2.80 |
| 17 | 140 | 48 | 12.8 | 64,600 | .197 | .0954 | .021 | 2.89 |
| 18 | 165 | 55 | 15.3 | 94,800 | .161 | .0718 | .020 | 3.01 |
| 19 | 150 | 50 | 25.0 | 58,900 | .425 | .0984 | .025 | 3.00 |
| 20 | 100 | 31 | 4.3 | 66,800 | .064 | .0607 | .016 | 3.24 |
| 21 | 90 | 32 | 4.3 | 66,900 | .064 | .0632 | .016 | 2.21 |
| 22 | 90 | 33 | 4.3 | 66,800 | .064 | .0642 | .016 | 2.75 |
| 23 | 115 | 40 | 2.9 | 101,700 | .028 | .0532 | .013 | 2.84 |
| 24 | 115 | 40 | 2.14 | 133,700 | .016 | .0393 | .011 | 2.84 |
| 25 | 115 | 37 | 4.03 | 198,300 | .022 | .0484 | .012 | 3.12 |
| 26 | 100 | 37 | 4.01 | 184,200 | .022 | .0484 | .012 | 2.70 |
| 27 | 60 | 24 | 1.01 | 366,300 | .003 | .0319 | .007 | 2.47 |
| 28 | 60 | 24 | 1.01 | 366,000 | .003 | .0323 | .007 | 2.44 |
| | | | | JP-5 Fuel | | | | |
| 29 | 225 | 72 | 10.8 | 21,700 | 0.497 | 0.0950 | 0.026 | 3.12 |
| 30 | 150 | 55 | 3.9 | 36,200 | .107 | .0720 | .018 | 2.74 |
| | | | | Benzene | | | | |
| 31 | 125 | 40 | 5.6 | 184,400 | 0.031 | 0.0532 | 0.013 | 3.08 |
| 32 | 70 | 24 | 1.4 | 357,100 | .004 | .0319 | .008 | 2.88 |
| | | | | Carbon tetrachloride | | | | |
| 33 | 140 | 56 | 9.6 | 79,500 | 0.121 | 0.0731 | 0.019 | 2.51 |
| 34 | 100 | 36 | 3.5 | 132,500 | .026 | .0475 | .013 | 2.76 |
| | | | | Water | | | | |
| 35 | 375 | 103 | 132.1 | 18,500 | 7.150 | 0.2022 | 0.052 | 3.64 |
| 36 | 250 | 68 | 40.5 | 33,200 | 1.220 | .1338 | .034 | 3.68 |
| 37 | 225 | 71 | 94.7 | 59,300 | 1.590 | .1393 | .036 | 3.18 |
| 38 | 200 | 60 | 49.4 | 59,300 | .835 | .1192 | .030 | 3.30 |
| 39 | 225 | 63 | 49.4 | 59,300 | .835 | .124 | .030 | 3.57 |
| 40 | 125 | 42 | 25.0 | 115,300 | .217 | .0837 | .022 | 2.94 |
| 41 | 75 | 25 | 6.1 | 230,600 | .027 | .0493 | .013 | 3.00 |
| 42 | 150 | 50 | 9.8 | 83,000 | .118 | .0656 | .018 | 3.00 |
| 43 | 315 | 85 | 27.1 | 49,700 | .547 | .1115 | .027 | 3.70 |

4453

TABLE IV. - COMPARISON OF EXPERIMENTAL RESULTS WITH

OTHER METHODS OF ATOMIZATION

| Type of atomization | Mean drop size | Related properties and exponents | Source |
|---|---|---|---|
| Crosscurrent breakup of liquid jets | $D_{30}$, or $\left(\frac{\Sigma nD^3}{\Sigma n}\right)^{1/3}$ | $\frac{(D_o)^{0.5}(\sigma)^{0.25}(\mu_l)^{0.25}}{(\rho_l)^{0.25}(V_s)^{0.75}(\rho_s)^{0.25}}$ | Eq. (10) |
| Pressure type (centrifugal nozzles) | $\frac{\Sigma nD^3 \log D}{\Sigma nD^3}$ | $\frac{(D_o)^{0.6}(\sigma)^{0.7}(\mu_l)^{0.2}}{(\rho_l)^{0.45}(V_l)^{0.45}}$ | Ref. 9; av. for 2 nozzles |
| Air atomization | $D_{32}$, or $\frac{\Sigma nD^3}{\Sigma nD^2}$ | $\frac{(\sigma)^{0.5}}{(\rho_l)^{0.5}(V_s)^{1.0}}$ | Ref. 4; for high ratio of air- to liquid-volumetric flow rates |

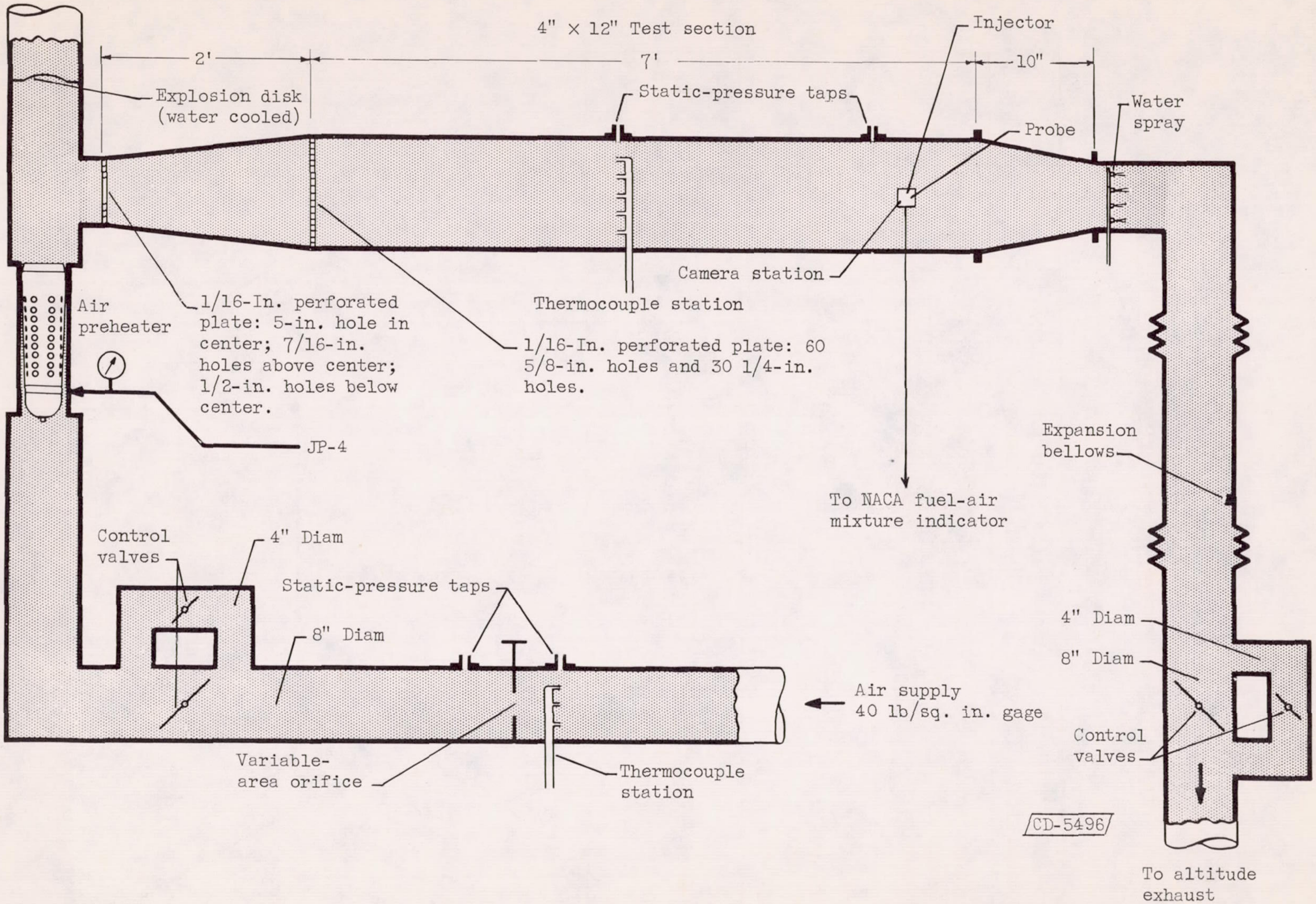


Figure 1. - Schematic drawing of test installation.

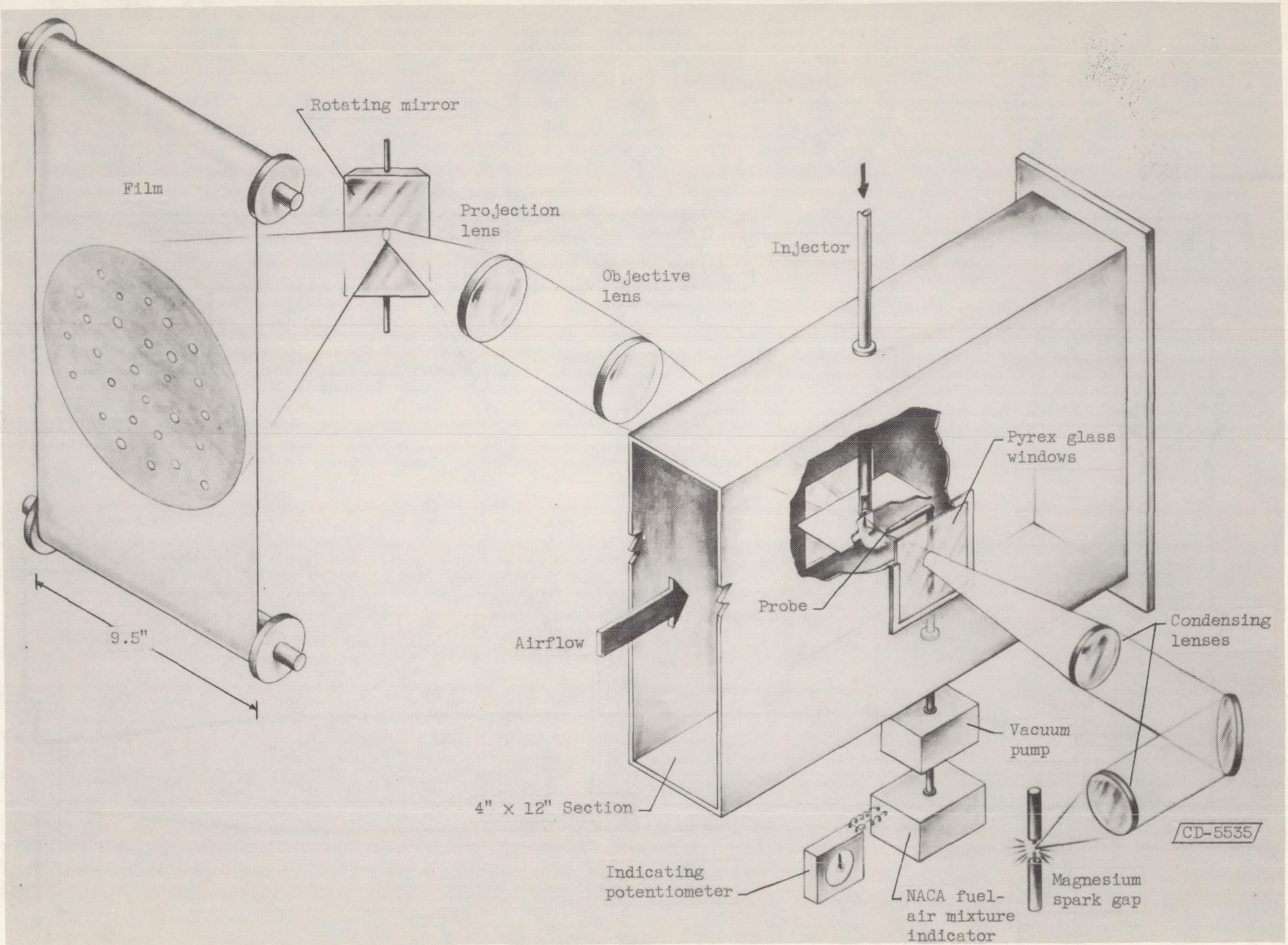


Figure 2. - Diagram of test section equipment and camera unit.

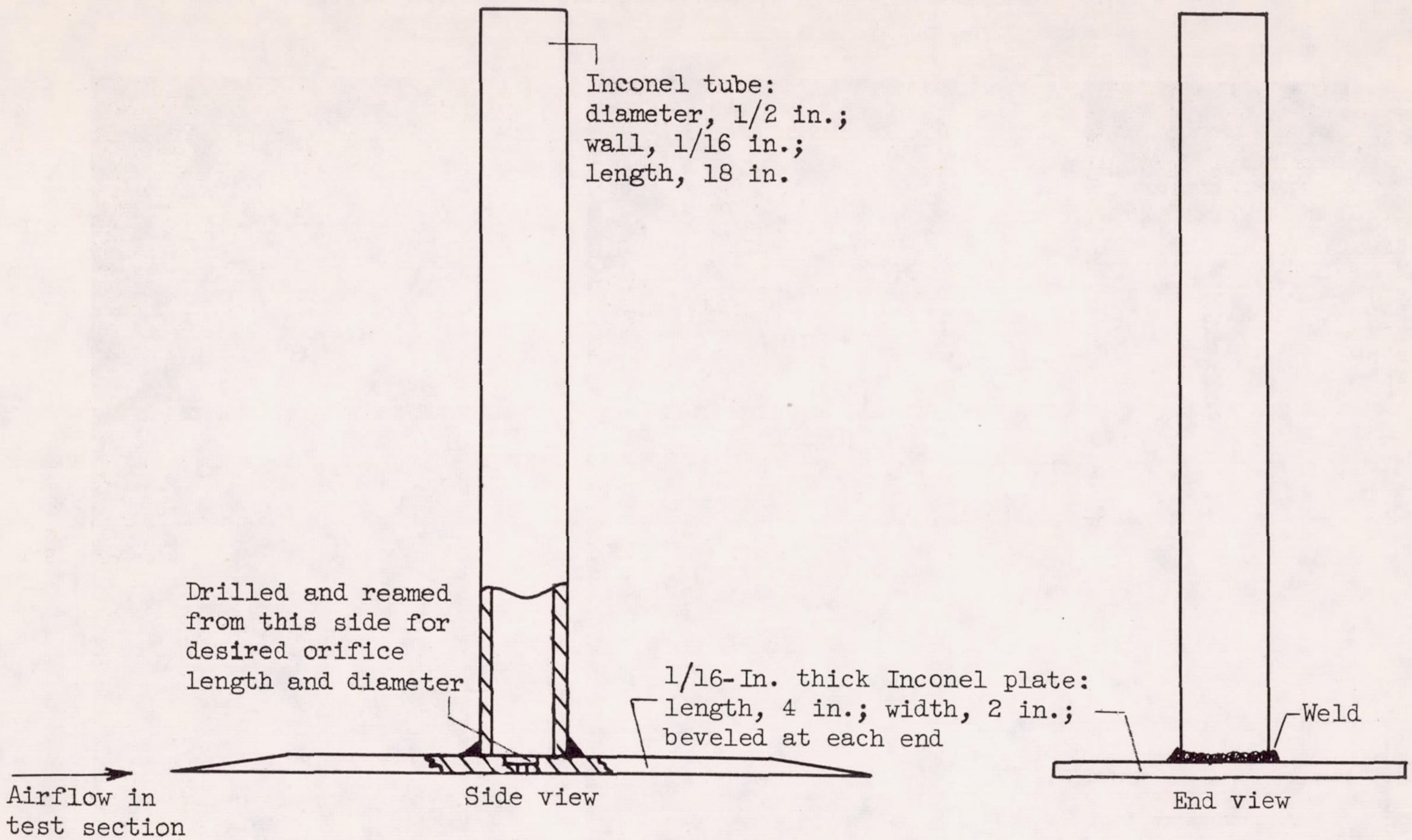


Figure 3. - Sketch of injector.

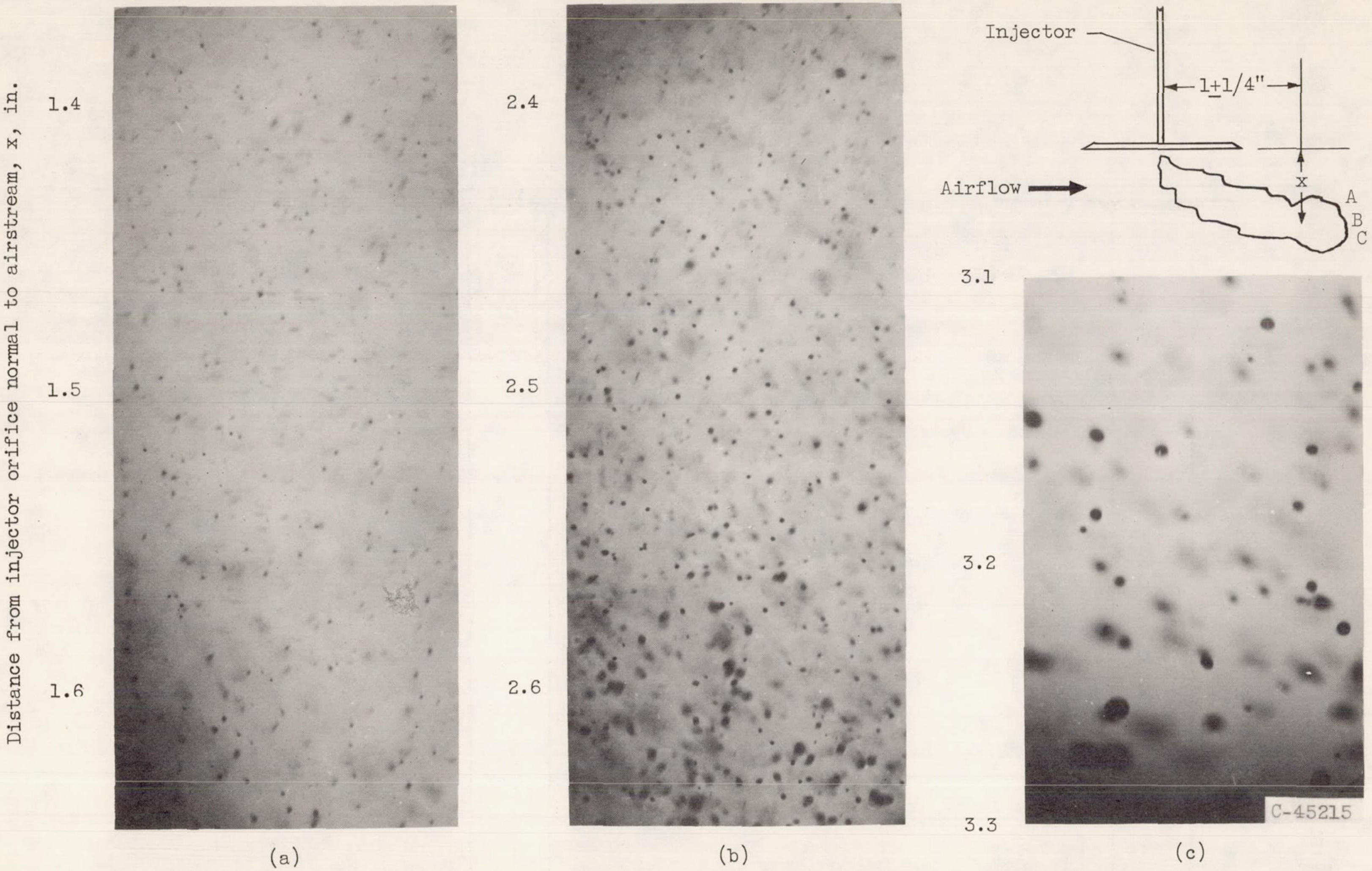


Figure 4. - Photomicrographs of isooctane spray in 100 feet per second velocity airstream. Magnification, 21:1; data, table I.

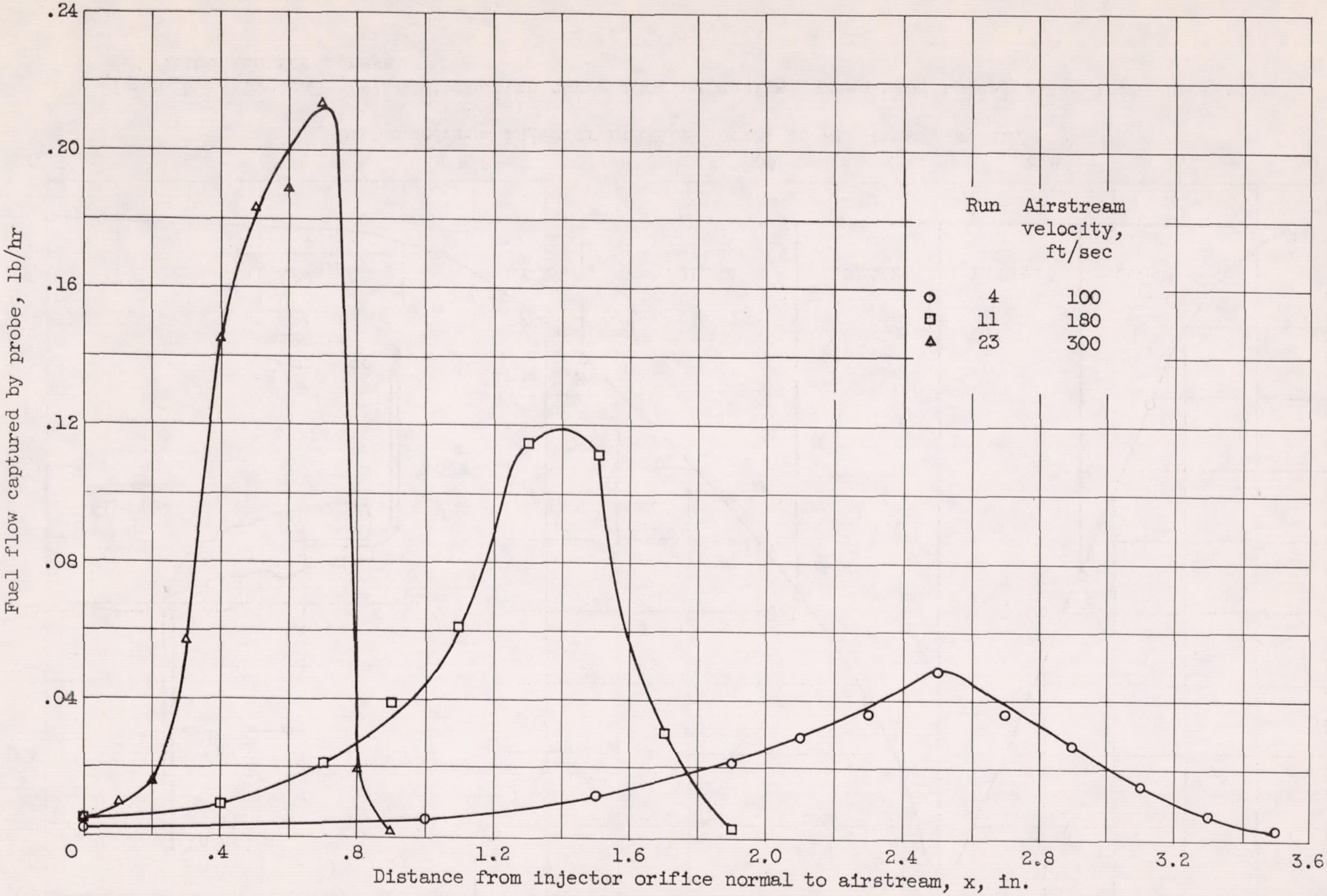


Figure 5. - Distribution of isooctane sprays normal to the airflow and 1 inch downstream from the injector. Orifice diameter, 0.030 inch; fuel jet velocity, 51 feet per second; fuel density, 42.6 pounds per cubic foot; air temperature, 86° F; air pressure, 29.3 inches of mercury absolute.

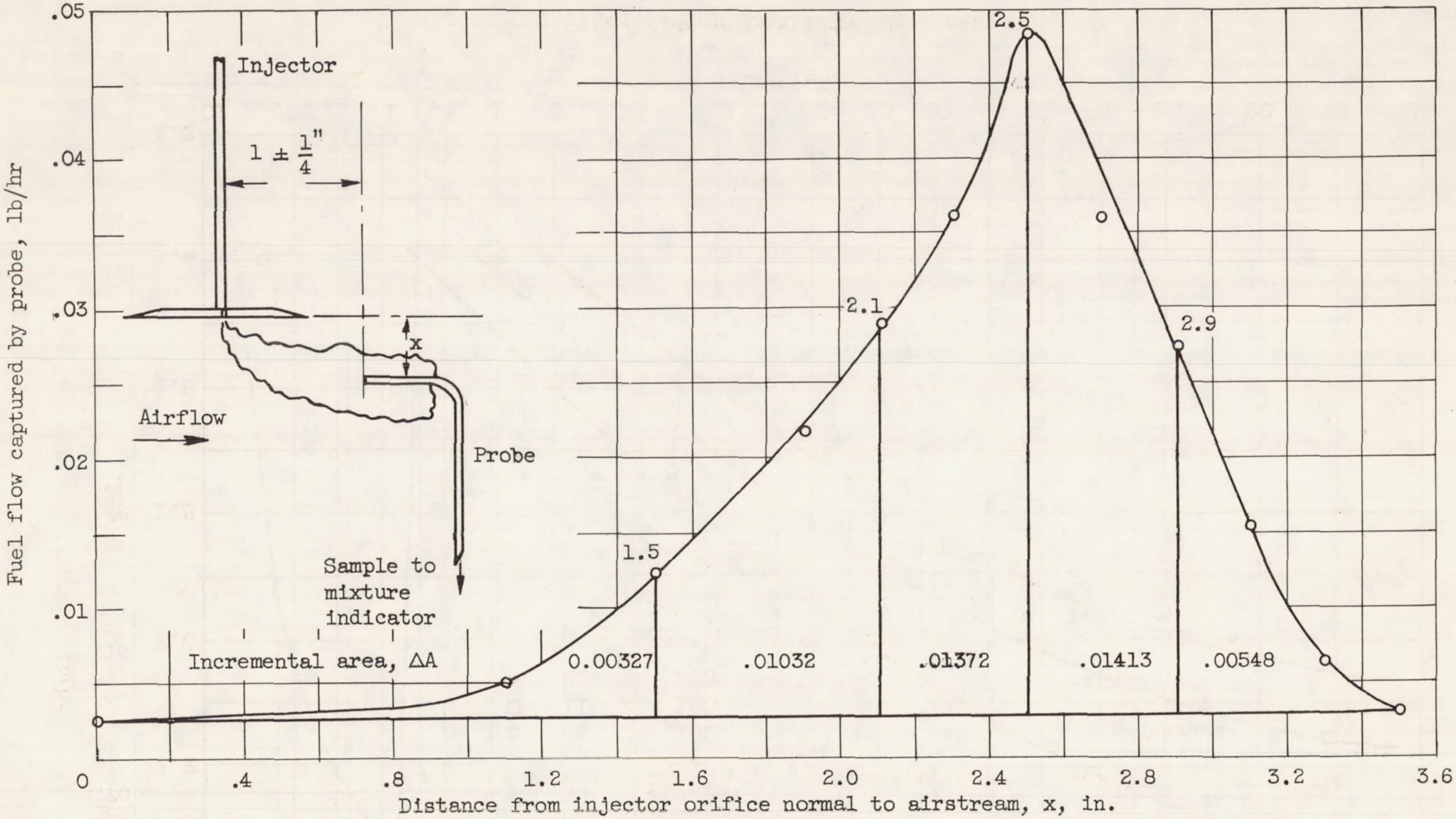


Figure 6. - Typical fuel distribution curve showing nominal areas used to calculate total drop-size distribution for sprays.

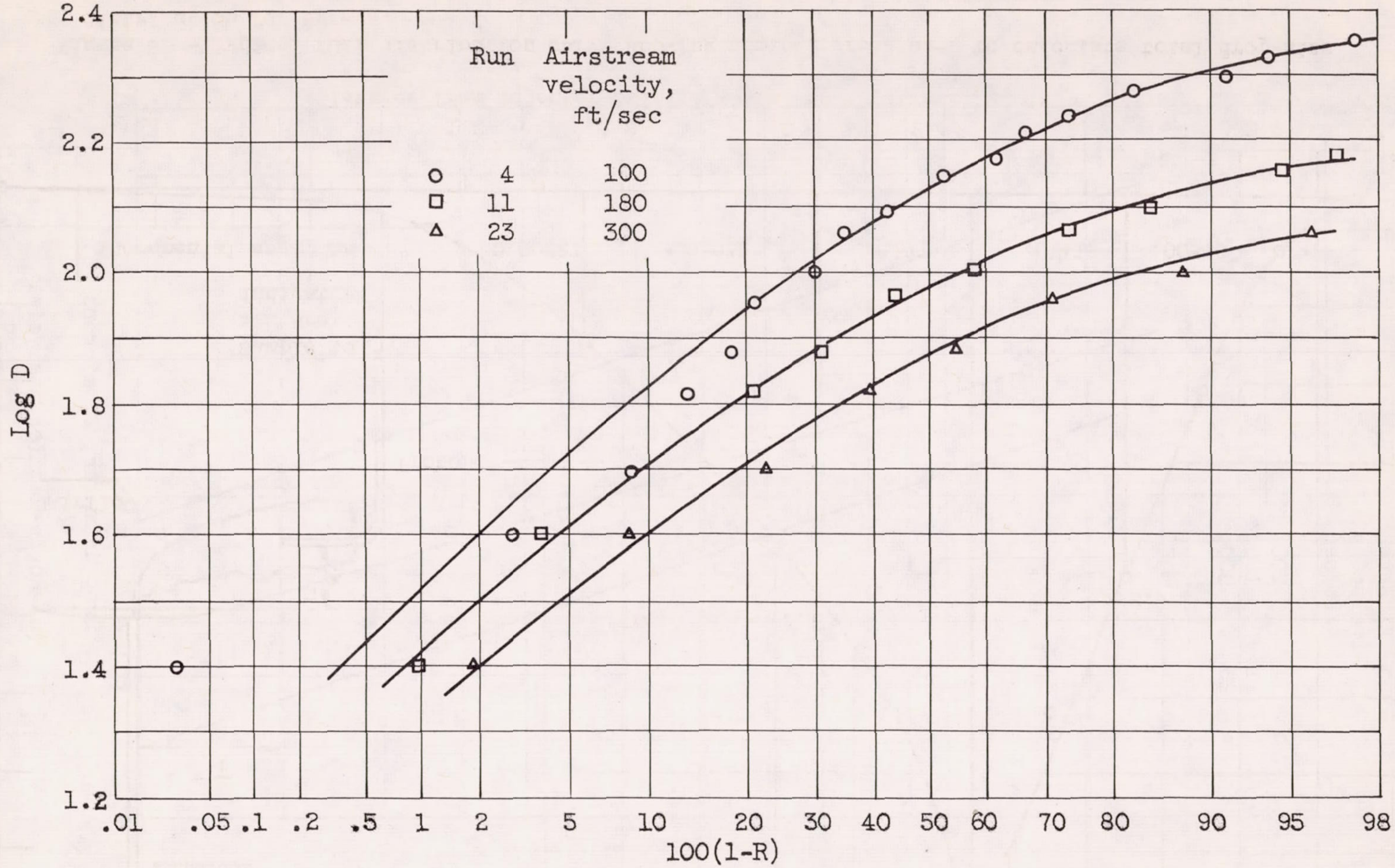


(a) Log-probability analysis.

Figure 7. - Effect of airstream velocity on atomization of crosscurrent isooctane jets.

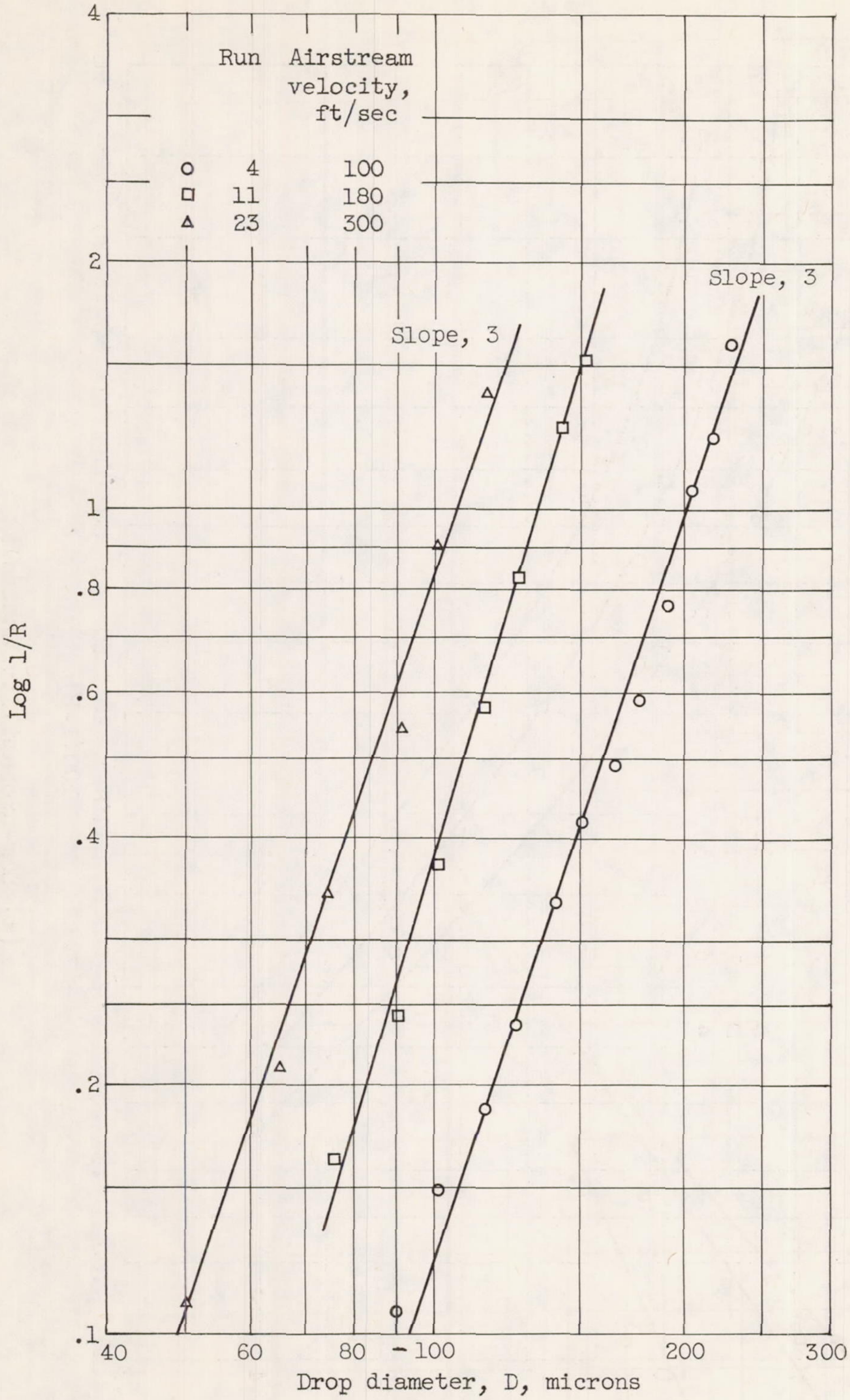


(b) Rosin-Rammler analysis.

Figure 7. - Continued. Effect of airstream velocity on atomization of crosscurrent isooctane jets.

4453

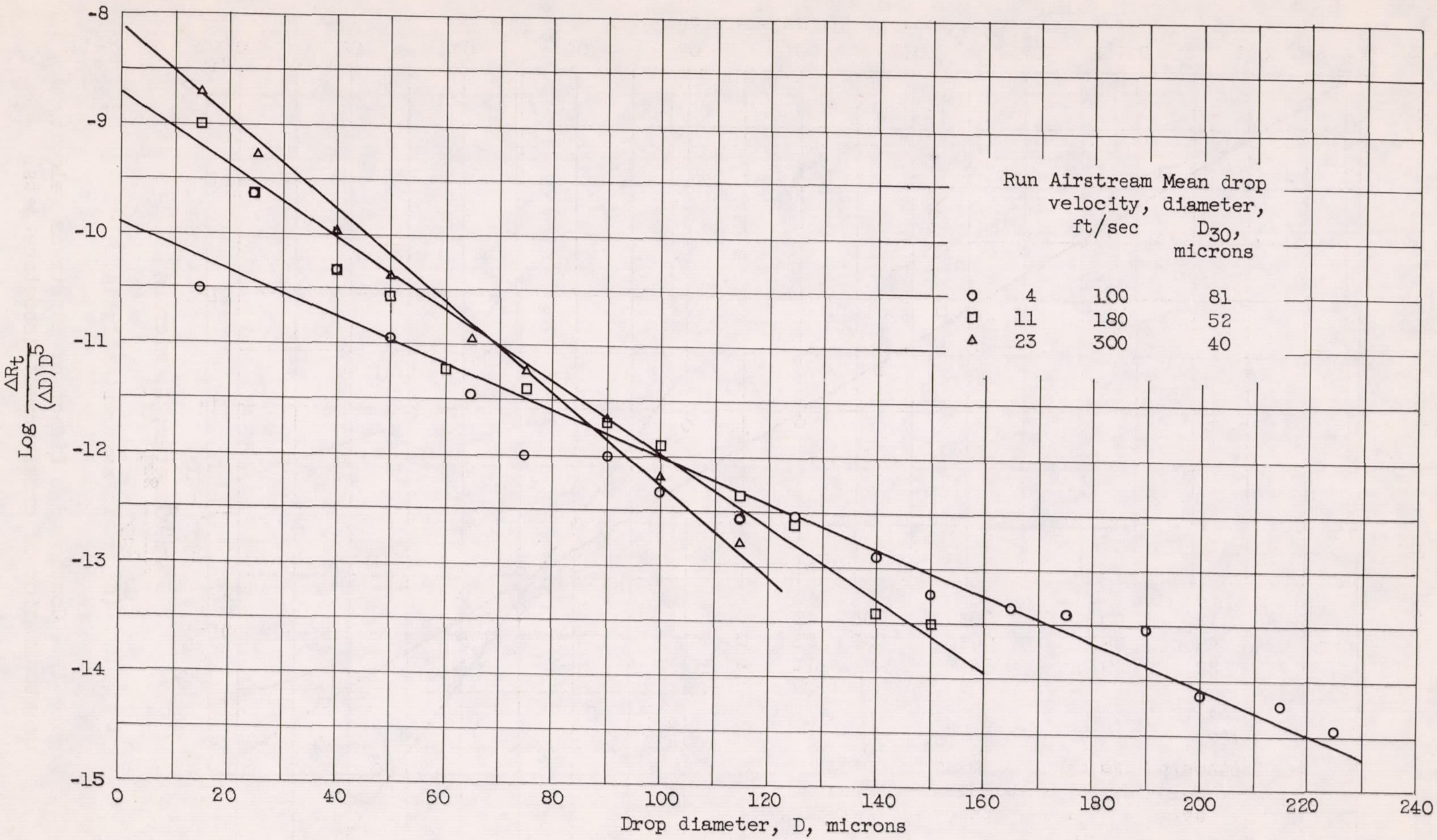


(c) Nukiyama-Tanasawa analysis.

Figure 7. - Concluded. Effect of airstream velocity on atomization of crosscurrent isooctane jets.

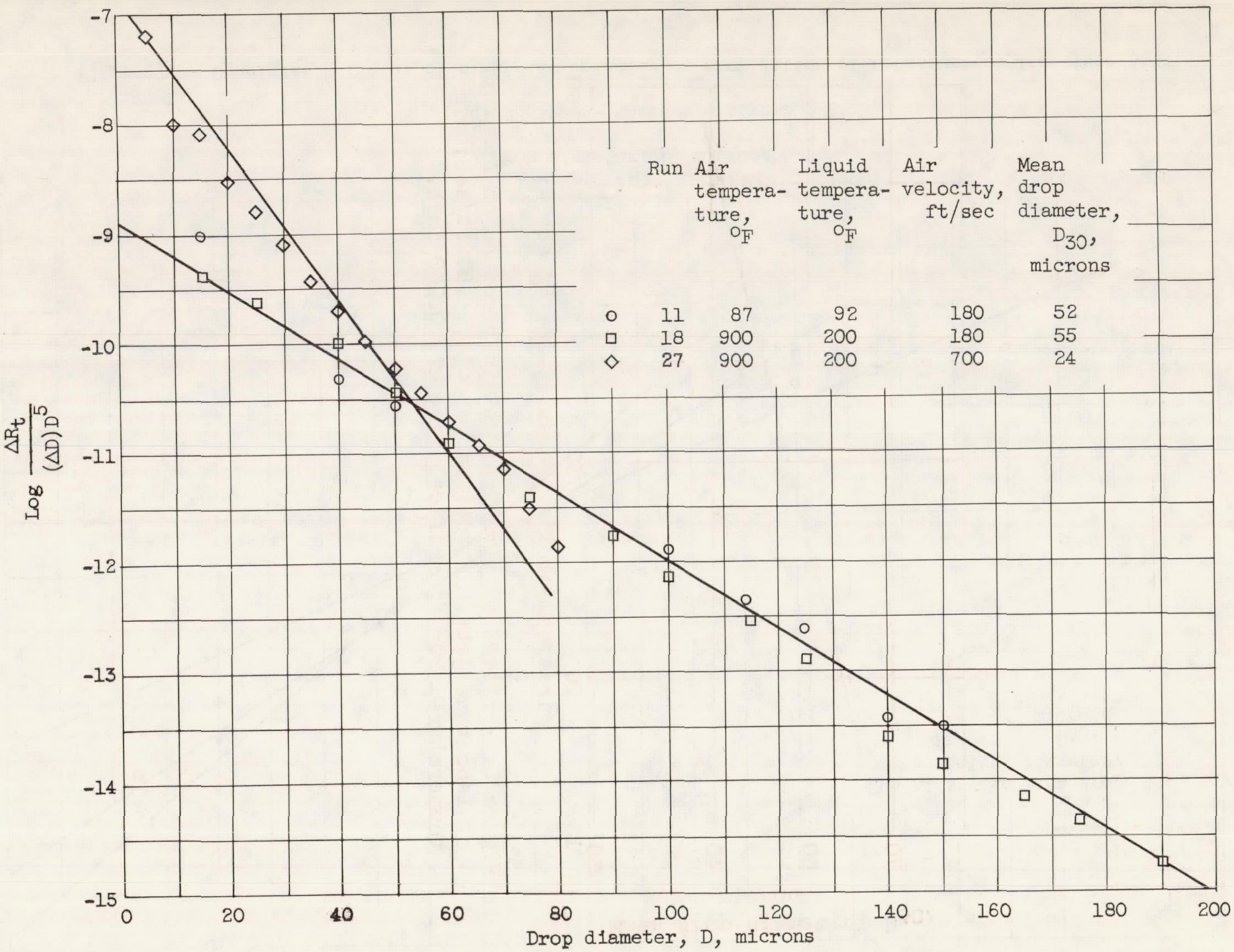


Figure 8. - Nukiyama-Tanasawa analysis showing combined effect of liquid and air temperature, and air velocity on atomization of crosscurrent isooctane jets.

4453

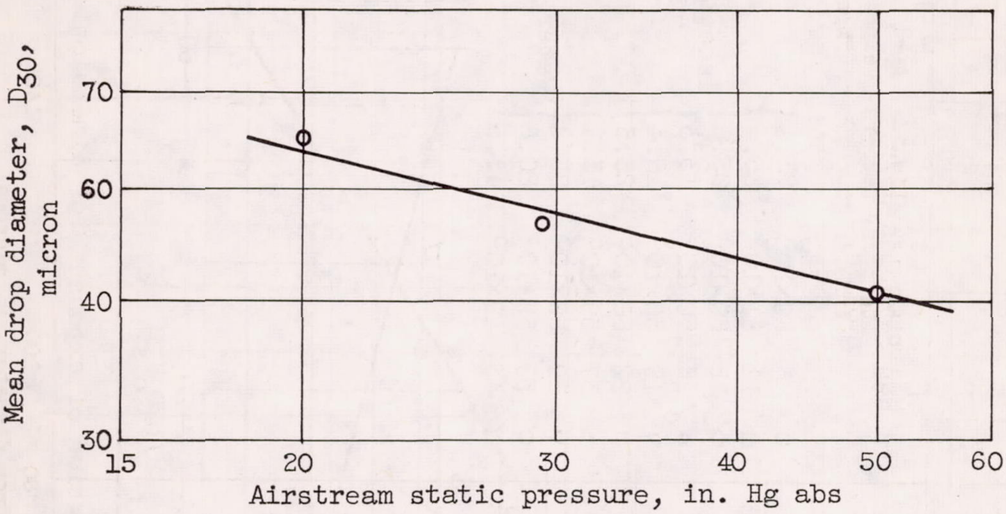


Figure 9. - Effect of airstream static pressure on breakup of isooctane jets. Airstream velocity, 180 ft/sec; air temperature, 90° F; orifice diameter, 0.030 inch.

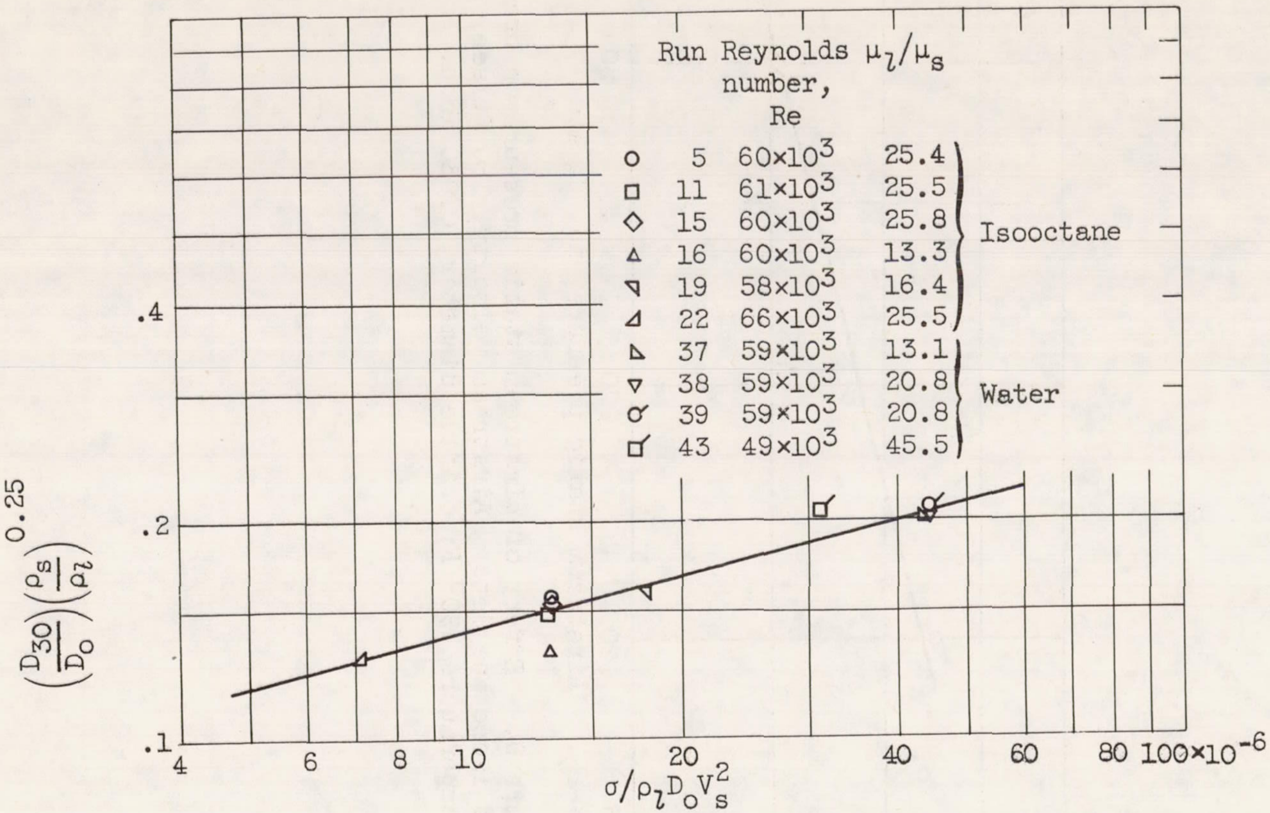


Figure 10. - Determination of exponent for dimensionless groups $\sigma/\rho_l D_o V_s^2$ and $\mu_l/\mu_s$.

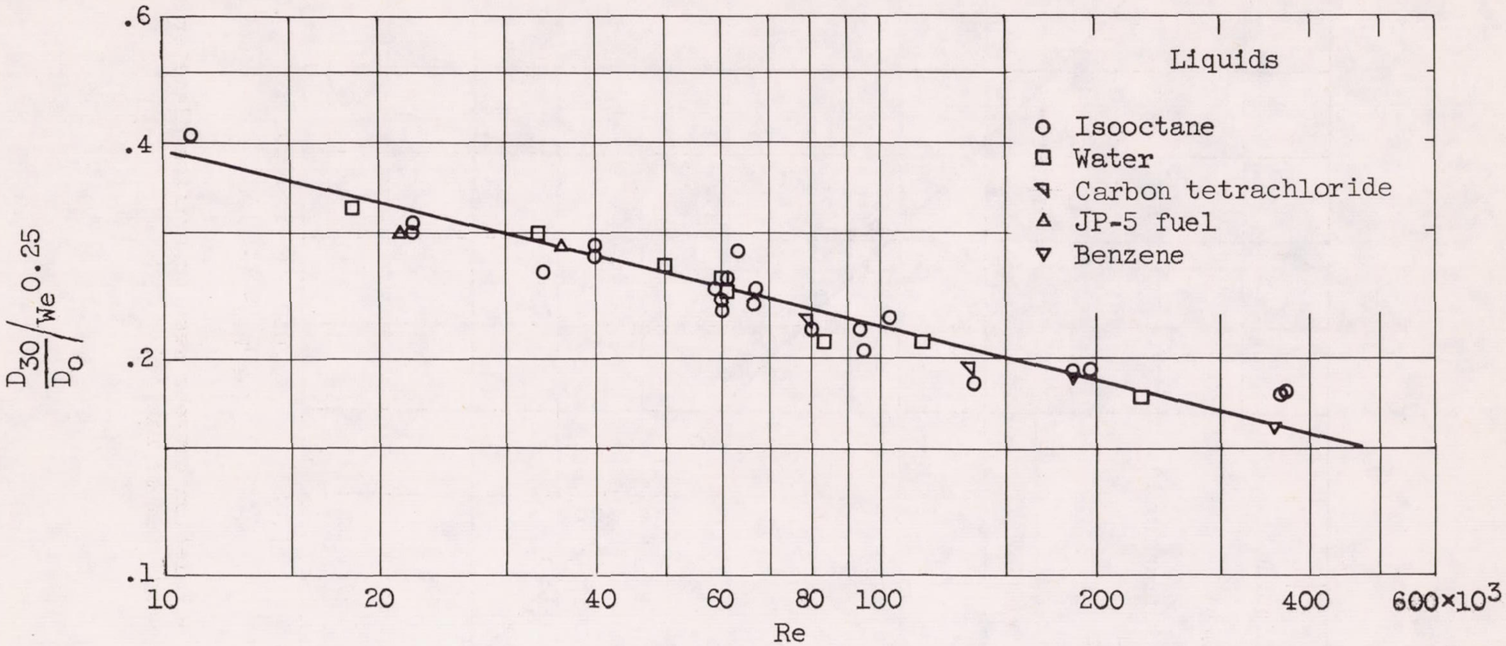


Figure 11. - Determination of Reynolds number exponent.

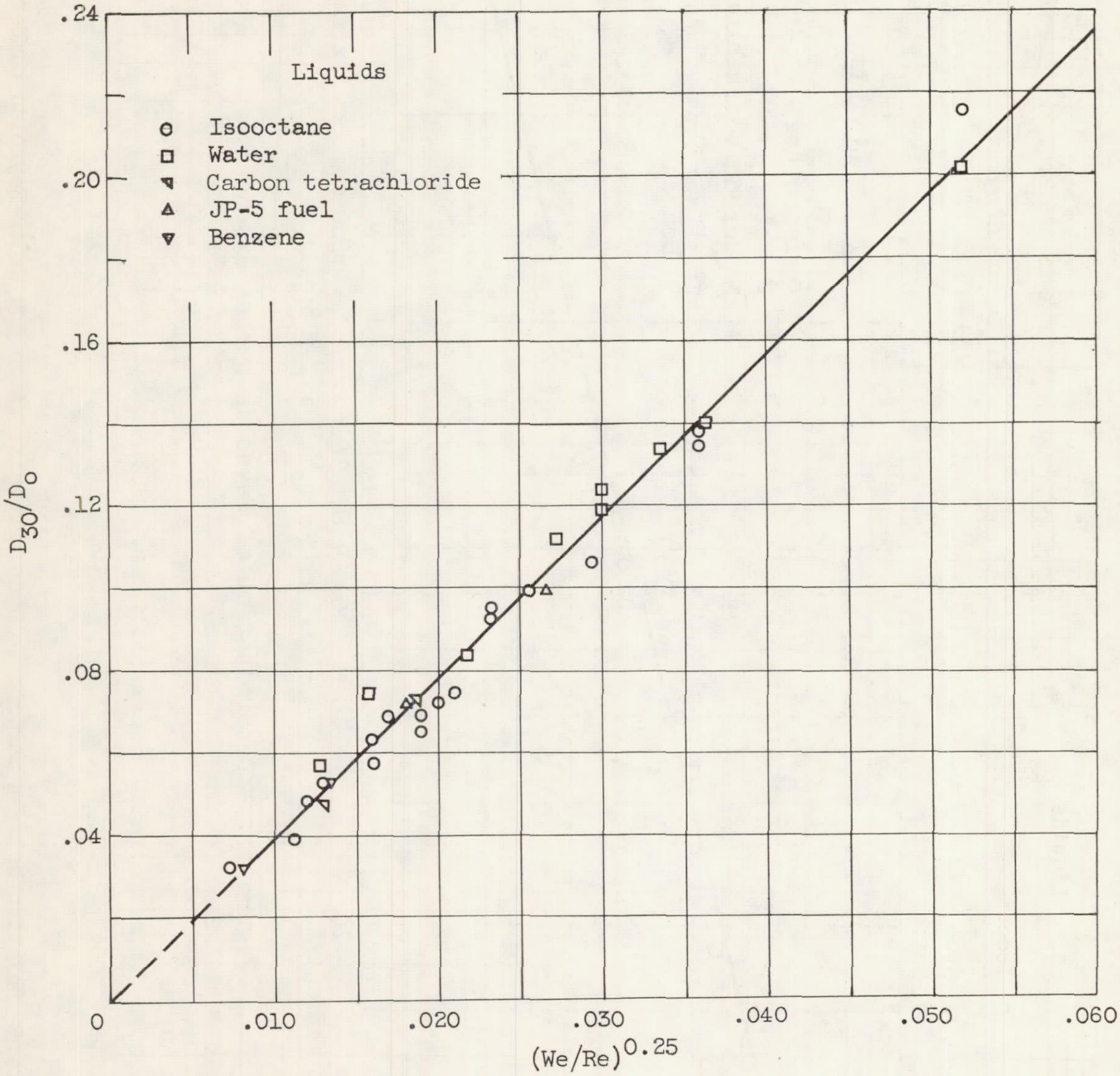


Figure 12. - Relation between mean to orifice diameter ratio and Weber-Reynolds number ratio.

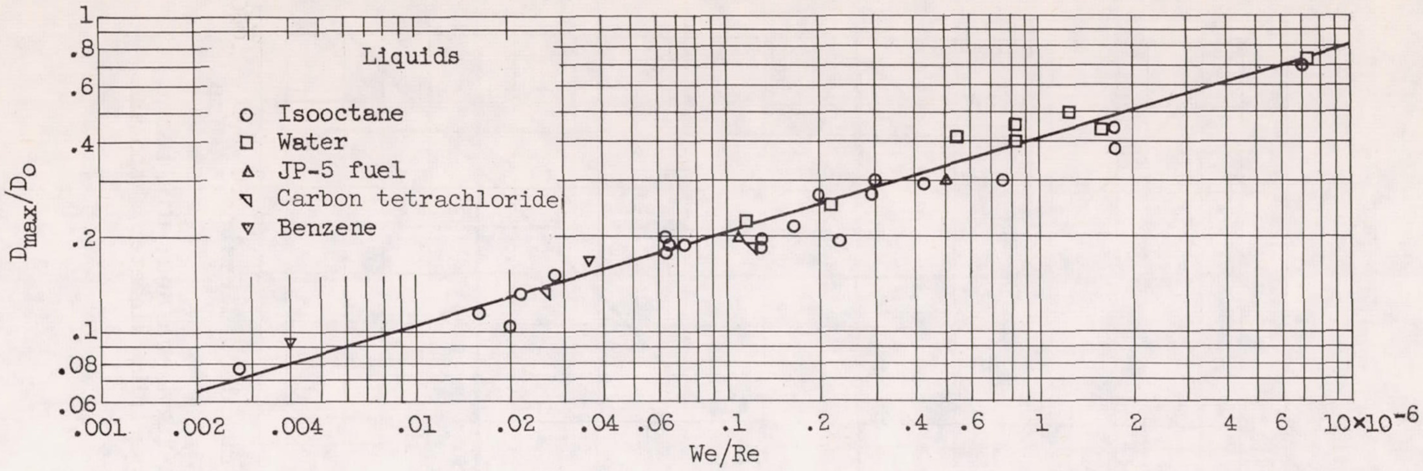


Figure 13. - Relation between maximum drop size to orifice-diameter ratio and Weber-Reynolds number ratio.

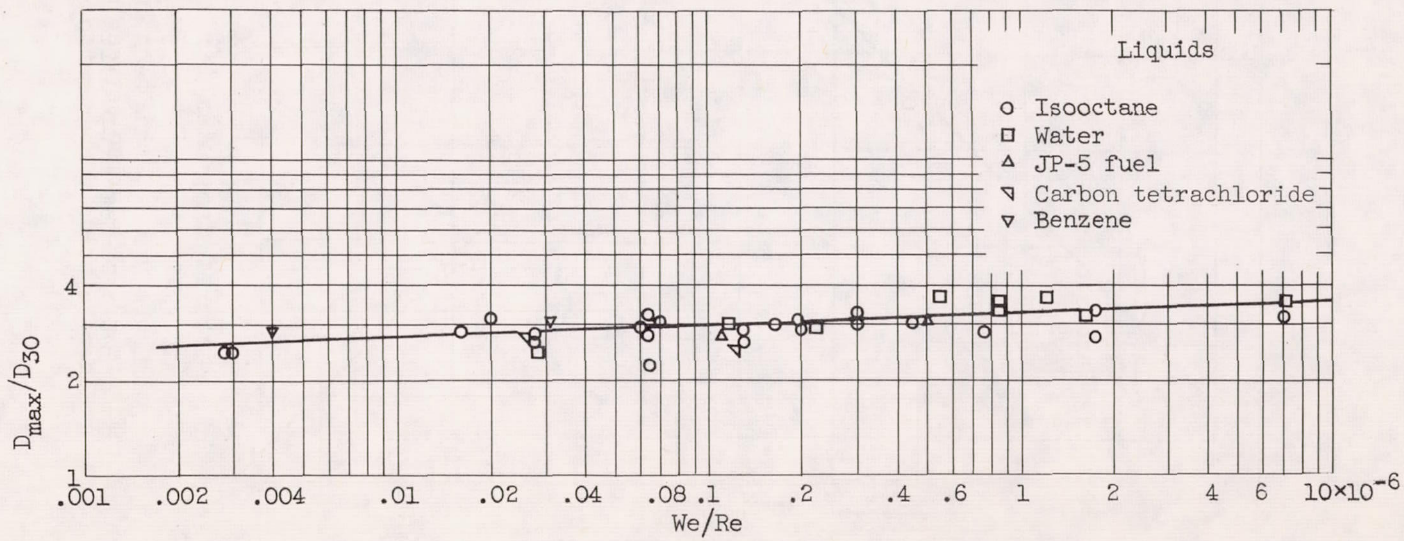


Figure 14. - Relation between maximum to mean drop-size ratio and Weber-Reynolds number ratio.

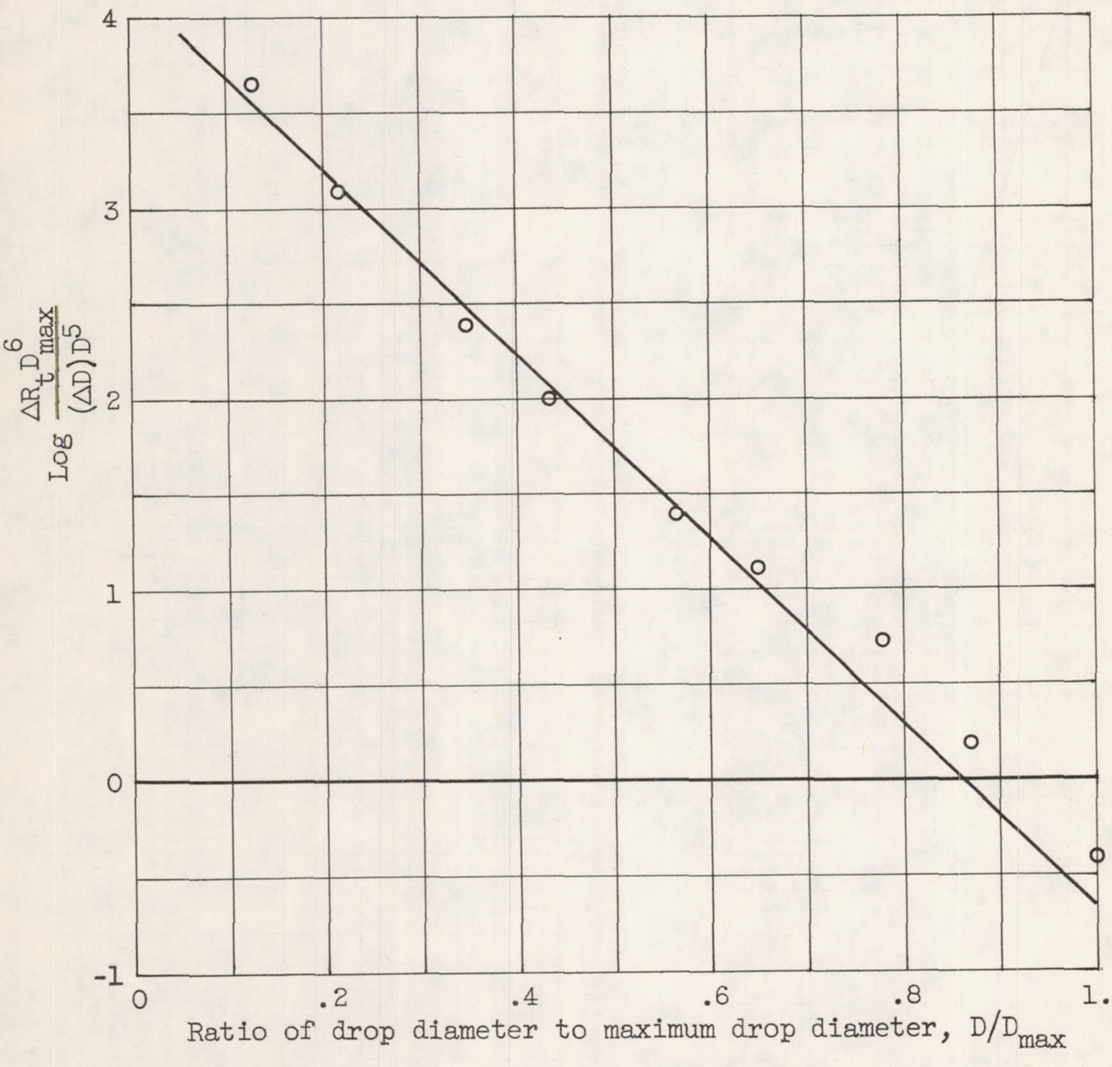


Figure 15. - Modified Nukiyama-Tanasawa analysis based on maximum drop size. Run 23.

NACA - Langley Field, Va.